

Quasi Periodic Oscillations in the Pre Phases of Recurrent Jets Highlighting Plasmoids in Current Sheet

Reetika Joshi, Ramesh Chandra, Brigitte Schmieder, Fernando Moreno-Insertis, Guillaume Aulanier, Daniel Nóbrega-Siverio, and Pooja Devi

Astronomy and Astrophysics (2020, submitted)

Overview

1. Introduction

- What is the trigger of the jets : emerging flux, instability, injection of helicity
- What is the possible interpretation of periodic oscillations : waves or plasmoids

2. Observations

- Six recurrent jets occurring in the active region NOAA 12644 on April 04, 2017.
- Data AIA filters, IRIS slit jaws.

3. Conclusion

- Good case–study to test the 2D and 3D magnetohydrodynamic (MHD) models that result from magnetic flux emergence ([Moreno-Insertis et al. \(2008, 2013\)](#), [Nóbrega-Siverio et al. \(2016,2018\)](#)).
- The pre-jet intensity oscillations have a period between 2 and 6 minutes, and are reminiscent of acoustic or MHD waves.

Introduction

- Solar jets are impulsive and well collimated plasma ejections observed along the whole solar cycle in a large wavelength range, from X-rays ([Shibata et al. 1992](#)) to the EUV ([Alexander & Fletcher 1999](#); [Innes et al. 2011](#); [Joshi et al. 2017](#)).
- Magnetic reconnection is believed to be the triggering mechanism behind the activation of jets. It can take place as a result of a process of magnetic flux emergence from the low solar atmosphere or interior. Observations indicate that the expansion of the magnetic flux emerging region leads to reconnection with the ambient quasi potential field and magnetic cancellation ([Schmieder et al. 1996](#); [Guo et al. 2013](#)). In the model by [Moreno-Insertis et al. \(2008\)](#), a split-vault structure is shown to form below the jet containing two chambers: a contracting and an expanding one. The volume of the chamber containing previously emerged loops is decreasing, while the volume of the chamber containing reconnected loops is increasing. This structure is also confirmed in radiation–MHD simulations by [Nóbrega-Siverio et al. \(2016\)](#).
- The jet evolution is preceded by some wave-like or oscillatory disturbances ([Pucci et al. 2012](#); [Li et al. 2015](#); [Bagashvili et al. 2018](#)) and these pre-jet oscillations are also driven by magnetic reconnection.
- We present a series of jets observed in the hot (EUV) channels with SDO/AIA and in cool temperatures with IRIS slit-jaw images from the AR NOAA 12644 on April 04, 2017. We study observation of pre-jet activity, in particular in the form of oscillatory behavior. We also find that this series of jet and surge observations fit completely with the expected behaviour predicted by emerging flux MHD models ([Nóbrega-Siverio et al. 2018](#)).

Observations

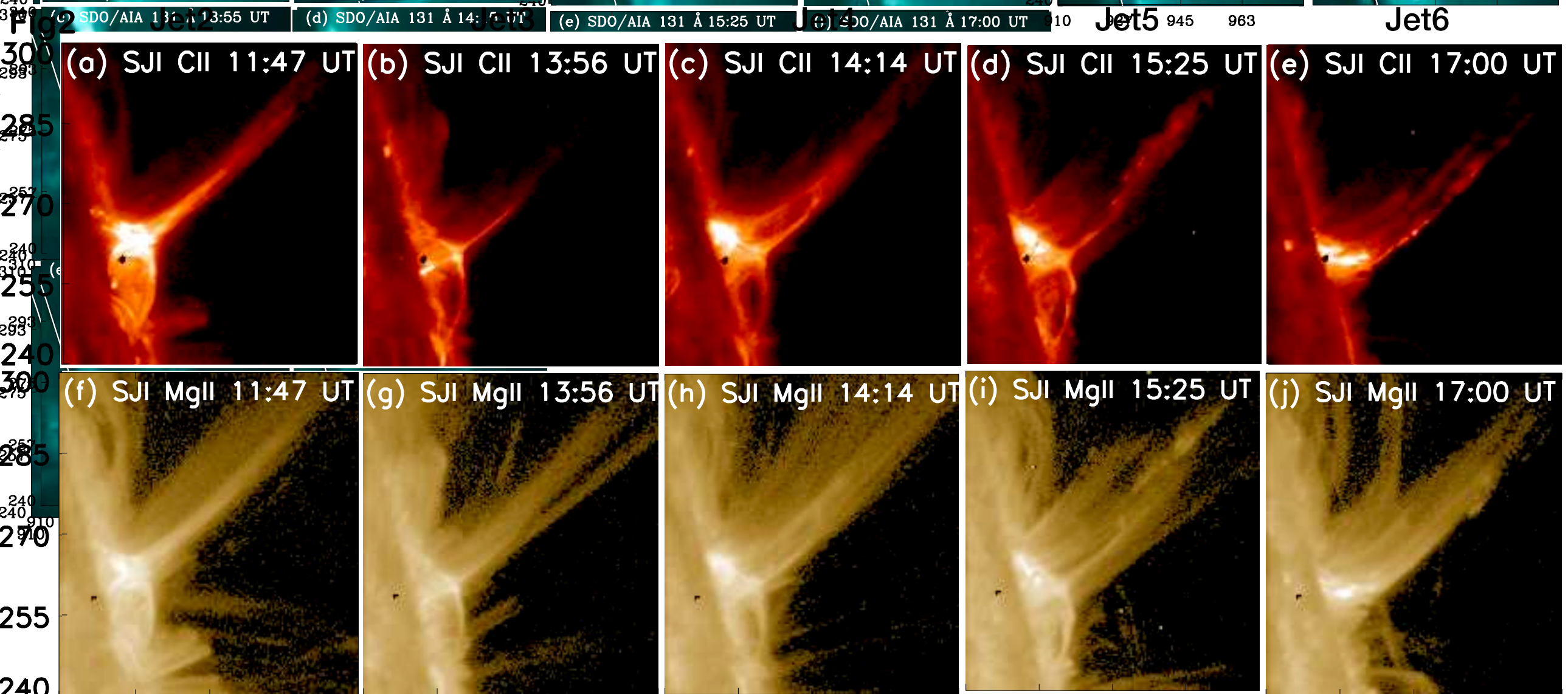
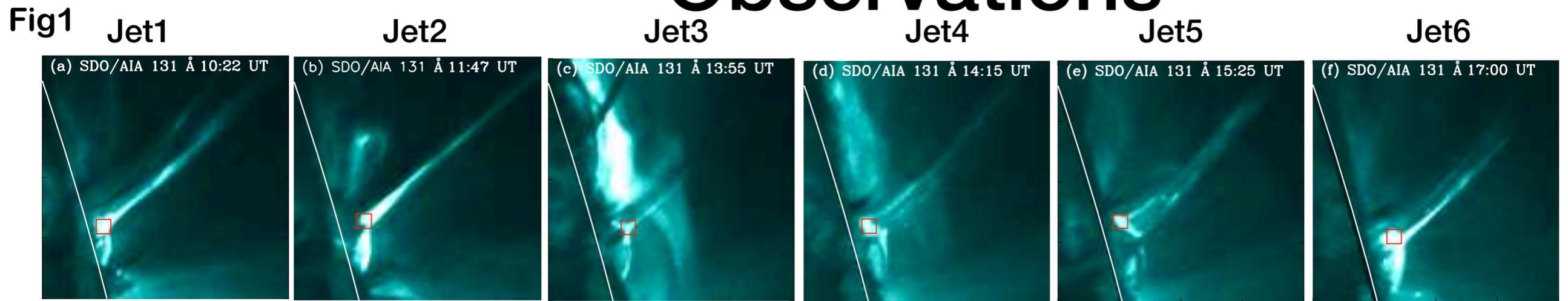


Fig1: Six solar jets (Jet1–Jet6) in SDO/AIA 131 Å filter. The red square in each panel shows the position at which the pre-jet oscillations are measured.

Fig2: IRIS observed the active region from 11:05 UT to 17:58 UT.

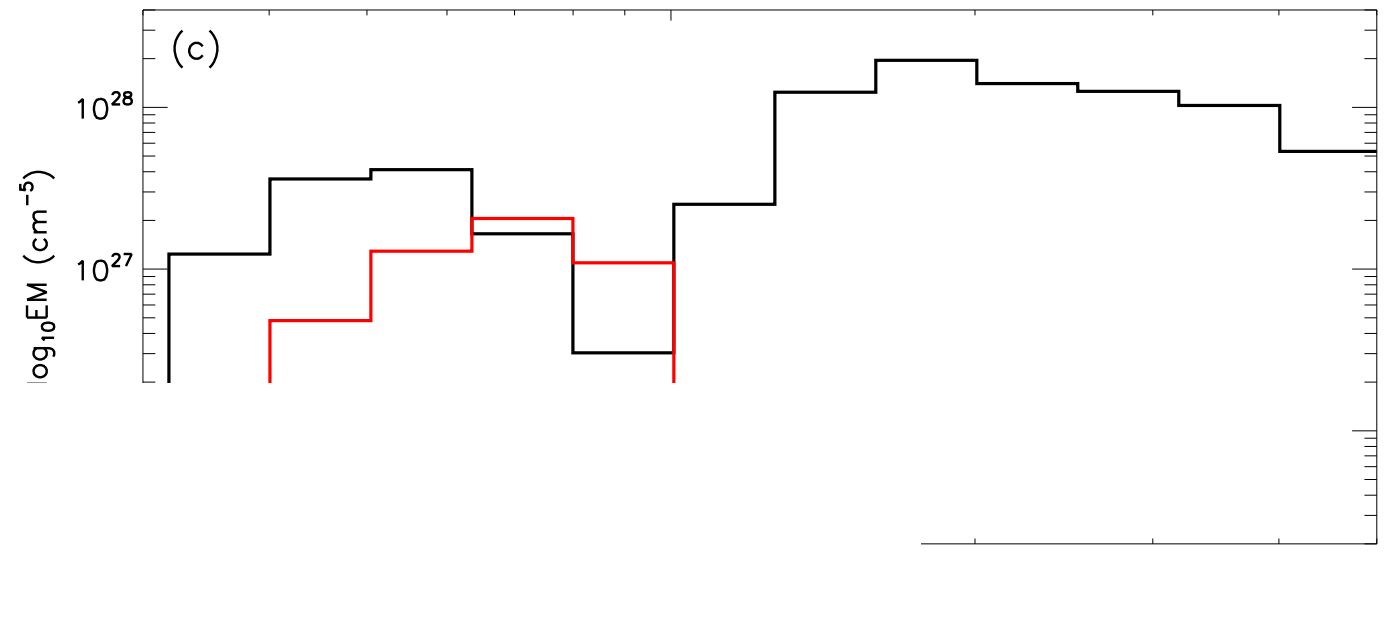
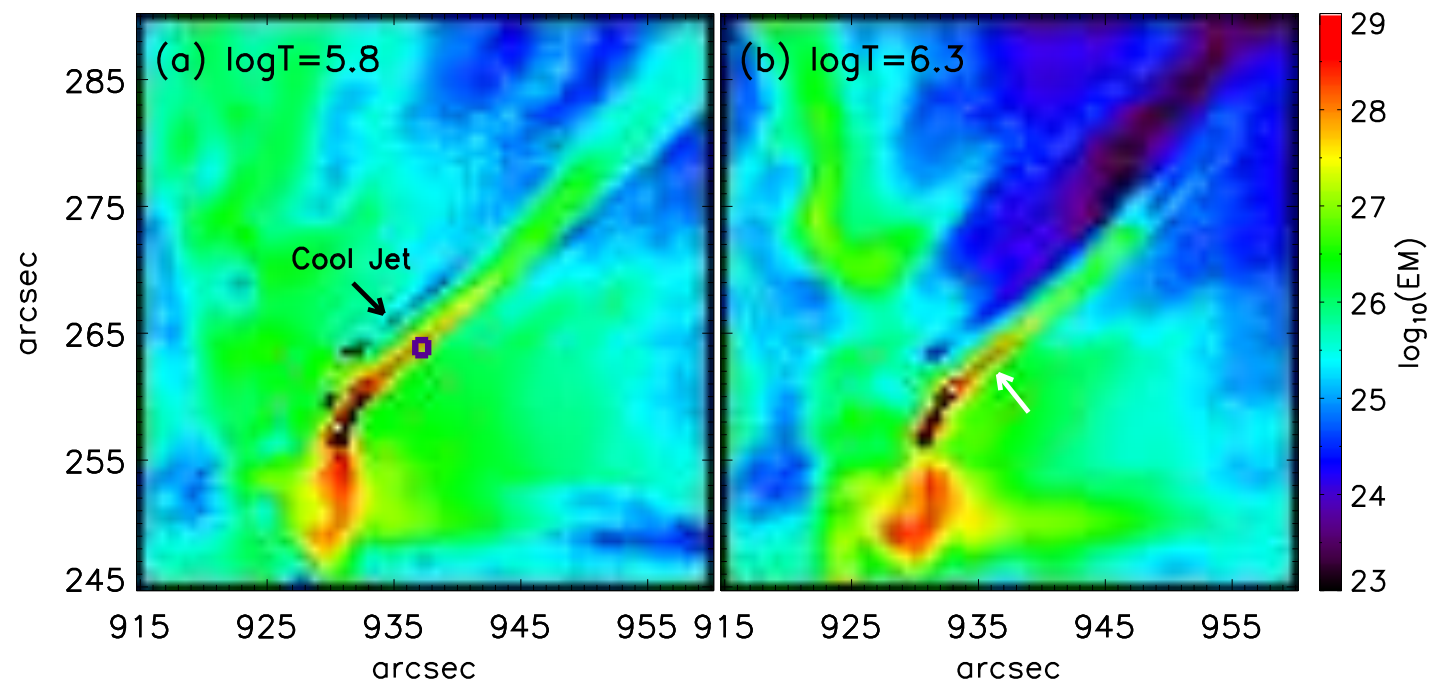
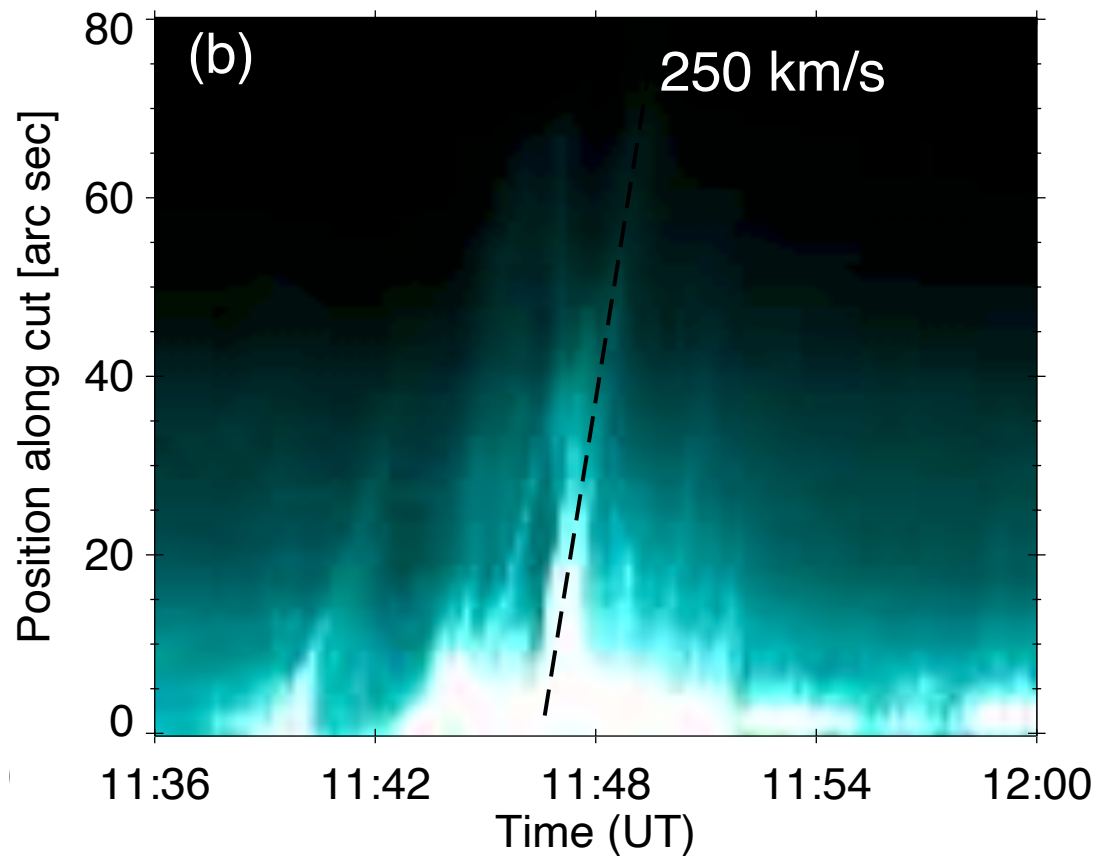
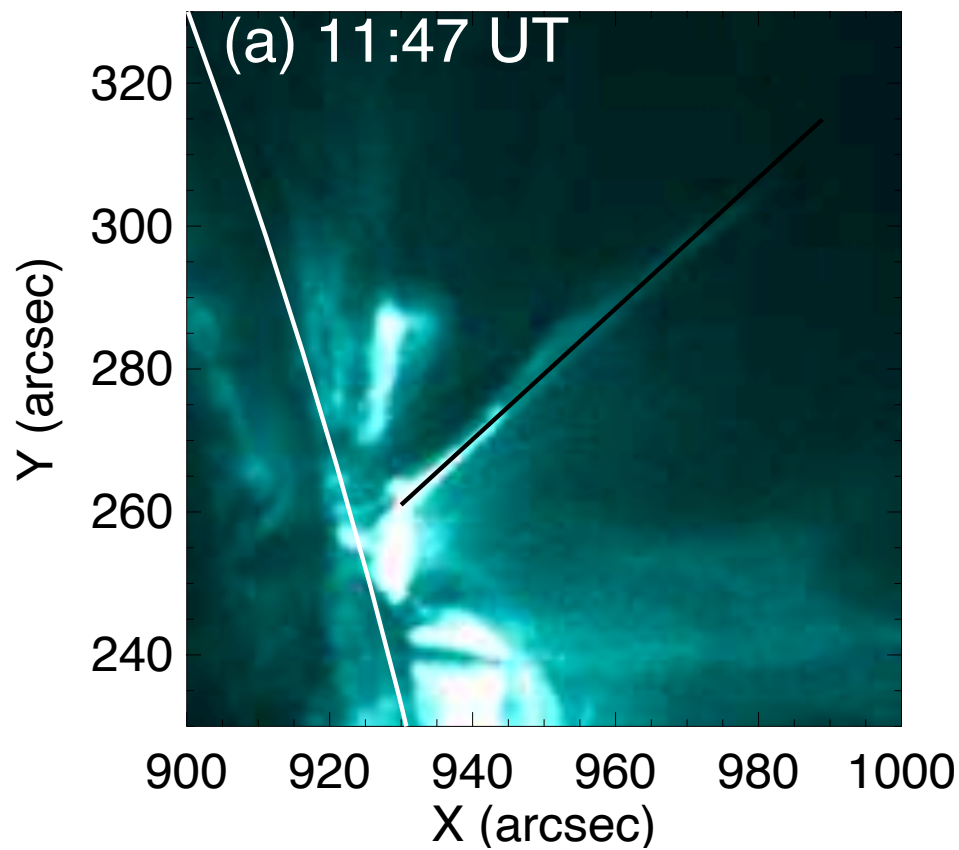


Fig4: Top: Two maps of Jet2, at two different temperatures. The blue square in panel (a) shows the location used for the emission analysis at the jet spire. White arrow in panel (b) shows the hot jet. Bottom: The red line shows temperature at the location of the blue box in panel (a) before the first jet and the black line shows the temperature of solar active region jet at 11:45 UT.

Fig3: An example of timeslice analysis of the jet 1, used for velocity and height calculations in AIA 131 Å. In panel (a) the solid black line is the slit location, which we use to make the height–time plot (b).

Intensity Distribution of Pre-phase of Recurrent Jets

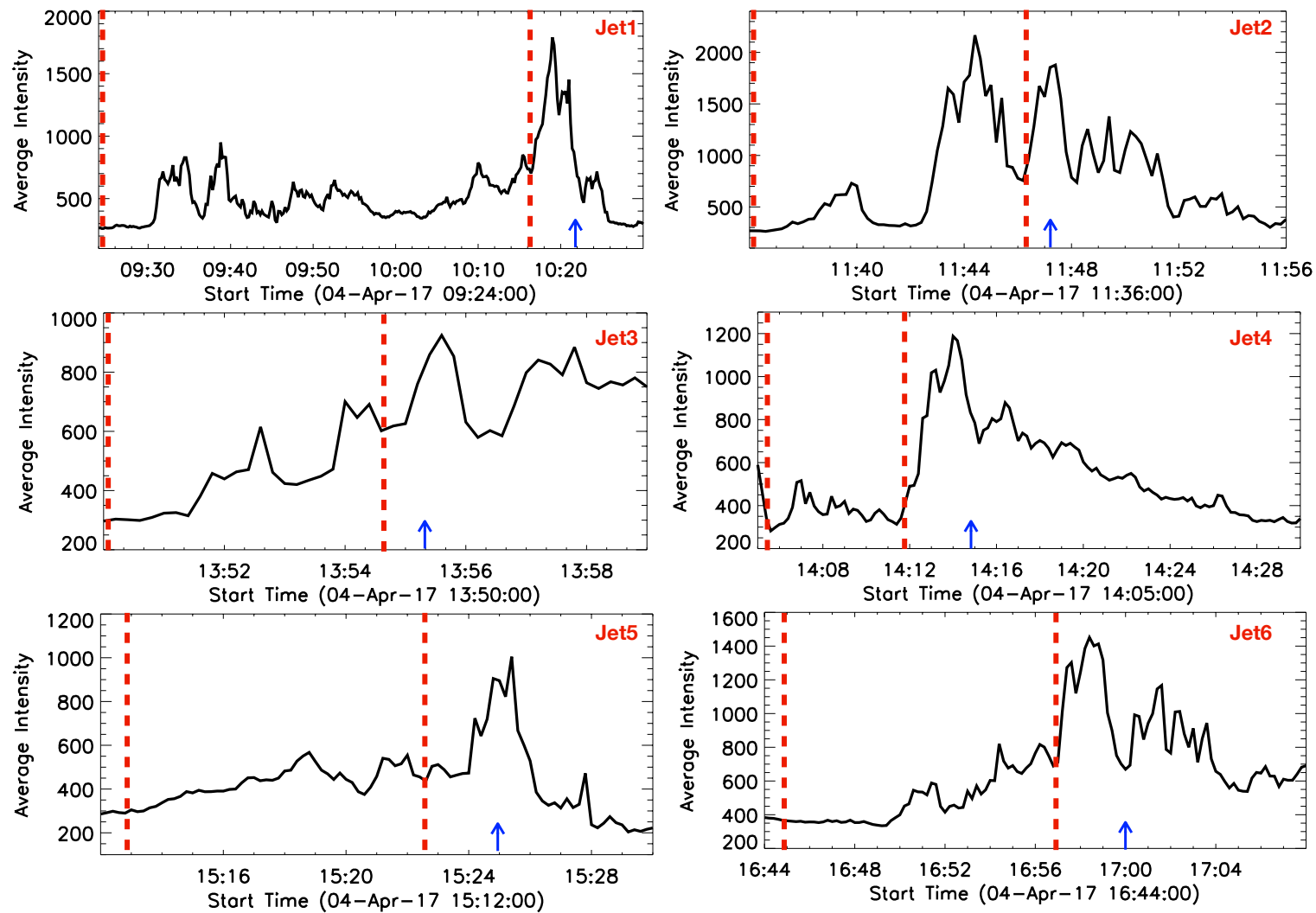


Fig5: Intensity distribution in AIA 131 Å during pre-phase of recurrent jets at the base of each jet. The location of the foot-point of each jet is displayed in Figure 1 (see red squares). The two vertical red dashed lines in each panel show the duration of the pre-jet intensity oscillation that is used for the wavelet analysis. The blue arrows show the peak phase of each main jet. Each small intensity peak before the main jet is related to a small jet ejection (10 Mm height) coming from the same location.

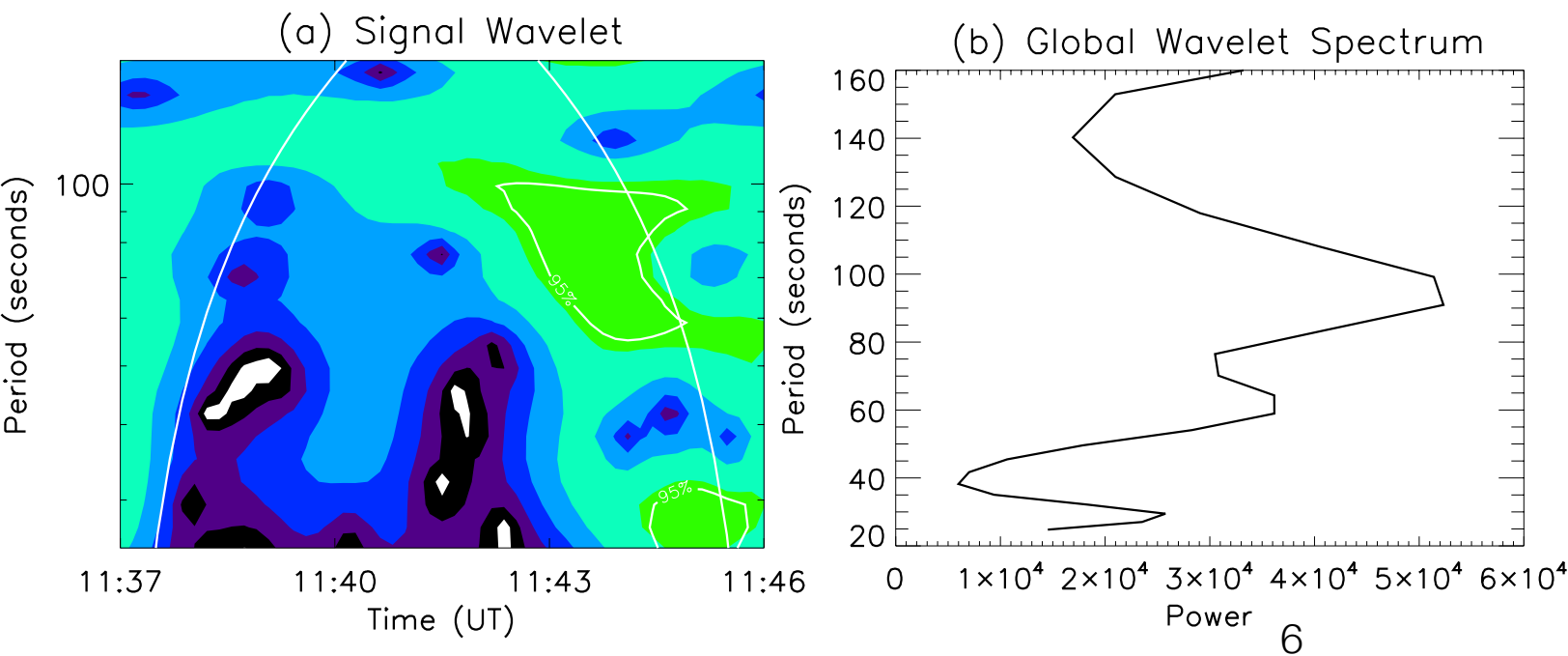


Fig6: Panel (a): An example of wavelet spectrum for the pre-jet intensity oscillations for Jet2. Panel (b): Global wavelet spectra for the distribution of power over time. The highest peak is corresponding to the time period of the pre-jet intensity oscillations, i.e. 1.5 min for Jet2.

Physical Parameters of Observed Jets

Jet no.	Jet start time (UT)	Jet peak time (UT)	Max height (Mm)	Average speed (km s ⁻¹)	T (MK)	EM (10 ²⁸ cm ⁻⁵)	Oscillation period (min)
1	10:15	10:22	80	210	1.4	1.4	6.0
2	11:46	11:47	50	245	1.8	1.9	1.5
3	13:54	13:55	40	265	1.4	1.5	2.5
4	14:12	14:15	50	250	1.8	1.1	2.0
5	15:23	15:25	55	235	1.8	1.3	4.0
6	16:57	17:00	70	220	1.8	2.0	2.5

Comparison Between Numerical Experiment and Observations

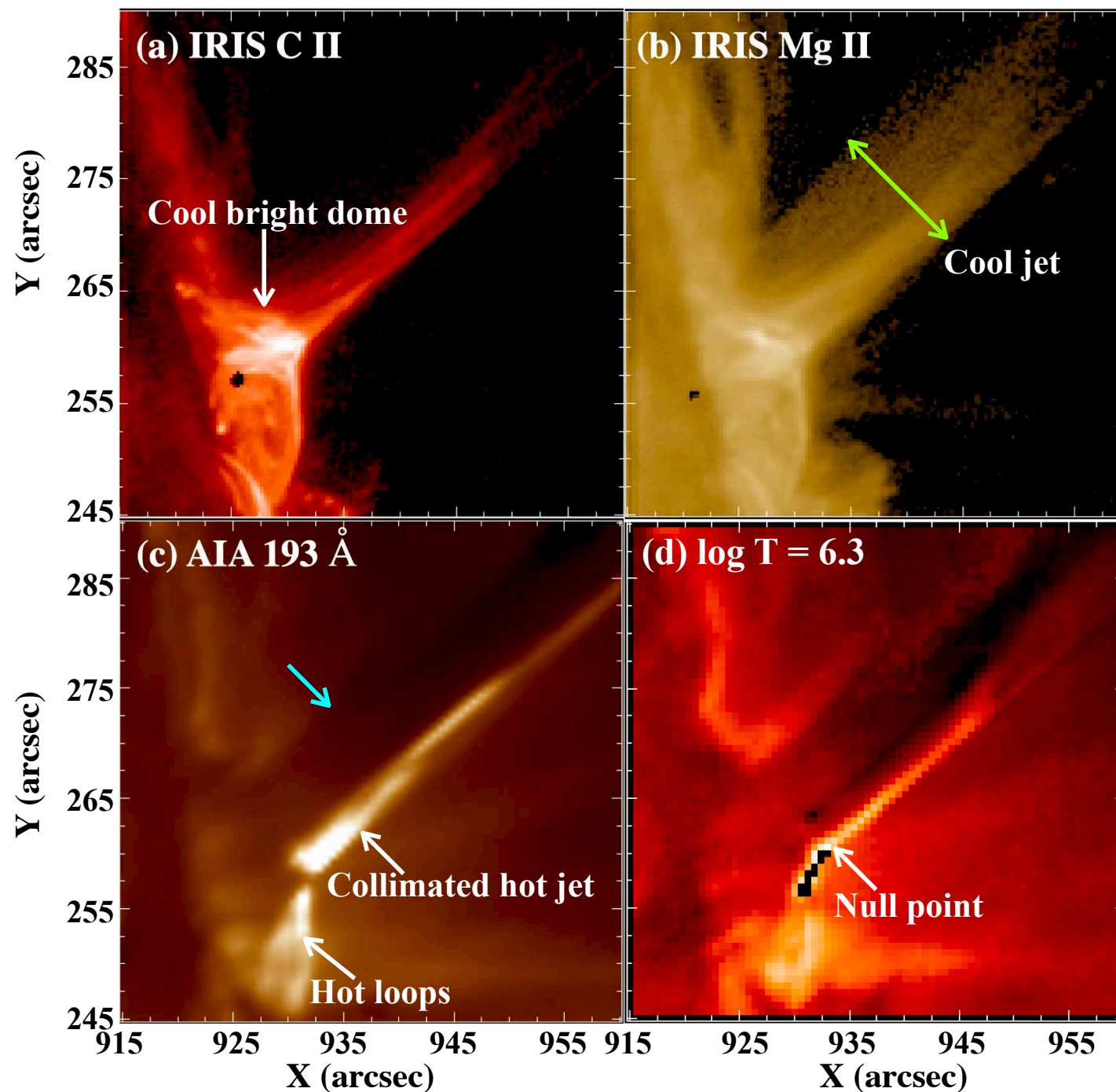


Fig7: Example of Jet2 at 11:45 UT observed with IRIS in panel a,b and AIA 193 Å in panel c. Cool bright dome in the northern side of the null point is shown with a white arrow in panel a. We note the broad cool jet in panel b (green arrow), the collimated narrow hot jet with hot loops (white arrows) and absorption area (cyan arrow) in panel c, the null-point and the current sheet (white arrow) in panel d. The black points are the saturated areas in panel d.

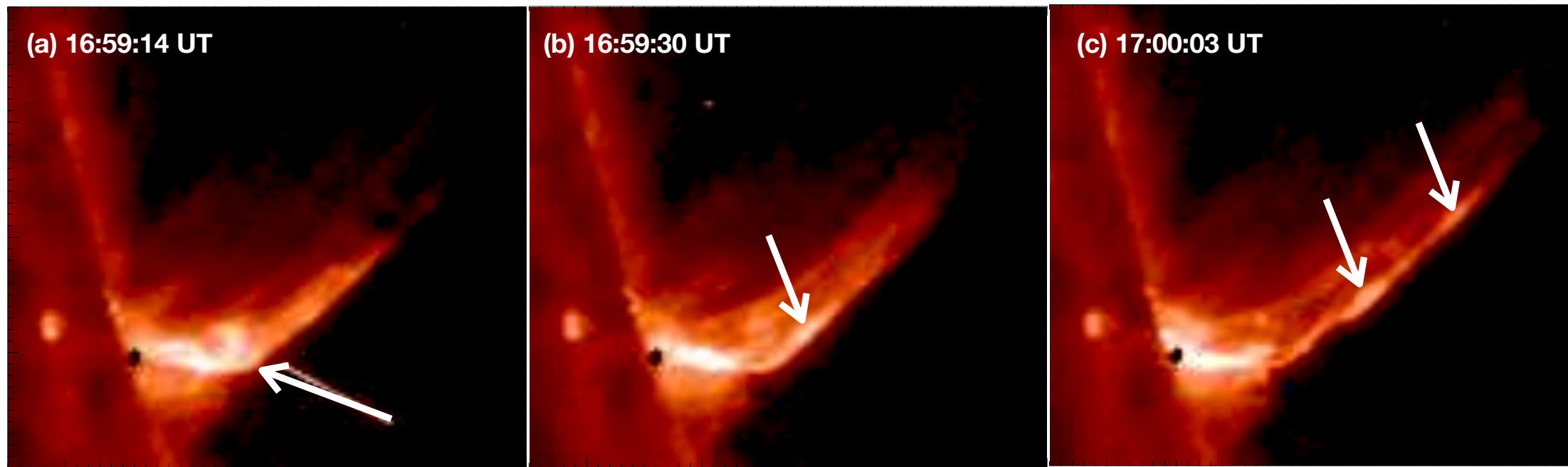


Fig8: Kernels of brightening moving along the Jet6 observed in the IRIS SJI in CII wavelength range (see white arrows). The kernels could correspond to untwisted plasmoids .

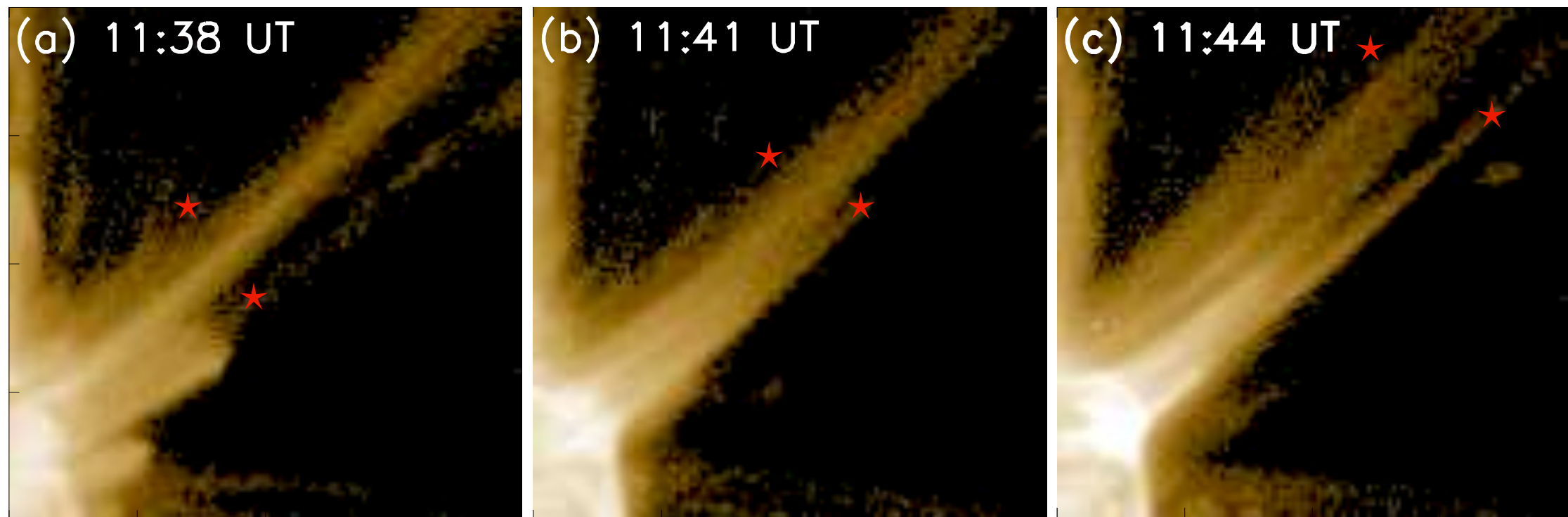


Fig9: The evolution of cool plasma material along both sides of the hot jet (Jet2) in IRIS MgII wavelength. The red star shows the leading edge of the cool material ejecting with an average speed of 45 km/s

Comparison Between Numerical Experiment and Observations

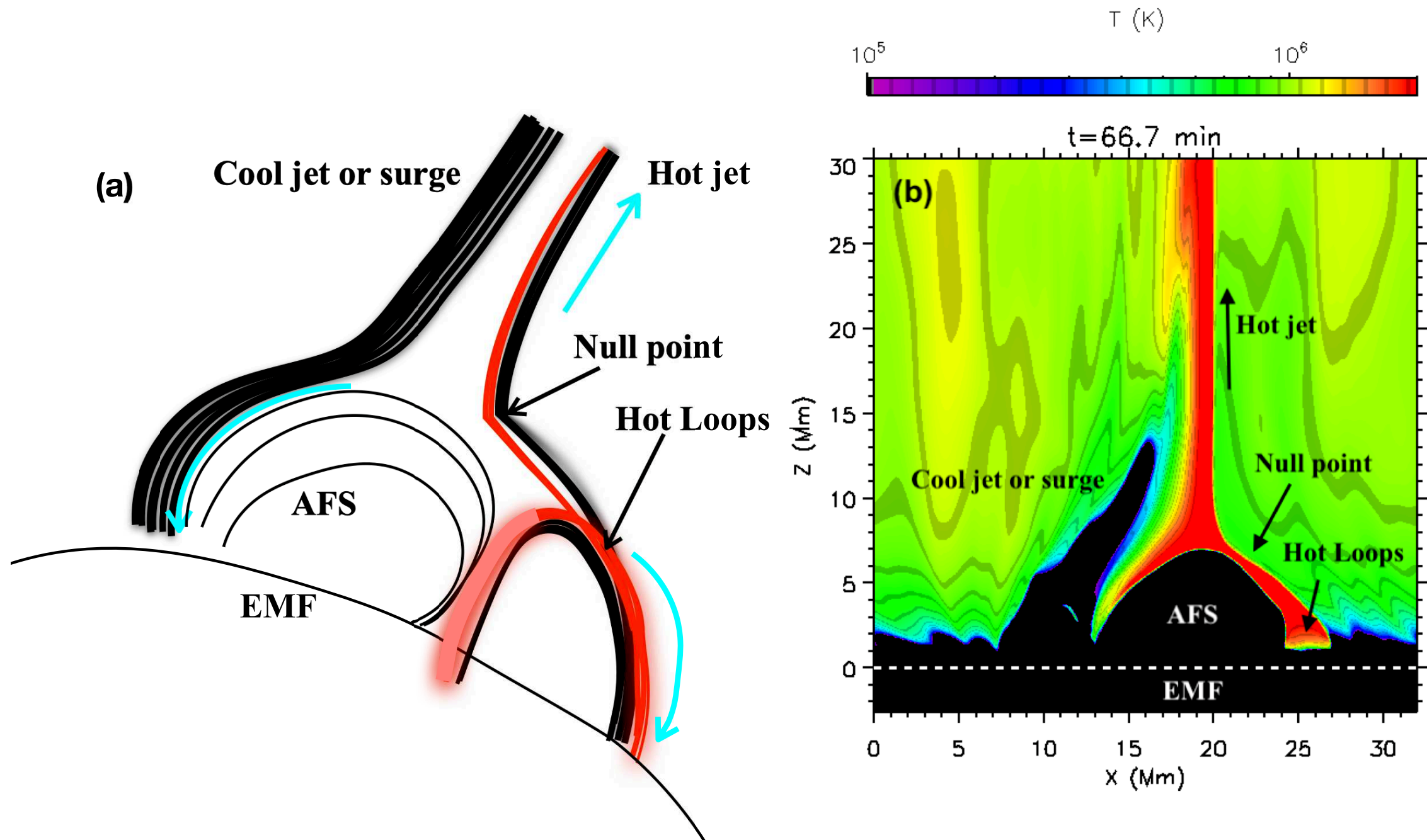


Fig10: Panel (a): Schematic view of the 3D jet derived from [Moreno-Insertis et al. \(2008\)](#), showing the location of the null point, the cool surge and the hot loops next to the AFS. The cyan arrows indicate the direction of the flows. Panel (b): Temperature map of one of the numerical experiments by [Nóbrega-Siverio et al. \(2017, 2018\)](#) showing the hot jet and the cool surge (an animation of this panel is available online). In both panels, the region of the convection zone where the new magnetic flux has emerged (EMF) is also indicated.

Summary

- All jets show pre-jet intensity oscillations at their base accompanied by smaller jets. The period of the oscillation ranges from 1.5 to 6 min.
- The jets are issued from a canopy-like structure with two vaults delineated by the brightenings seen in the different wavelengths. One of the vaults harbors hot loops as seen in the EUV AIA filters and also in IRIS CII wavelength.
- The spatial and temporal pattern of brightenings in the various wavelengths show clear similarities with the two- and three-dimensional numerical models of [Moreno-Insertis et al. \(2008\)](#); [Moreno-Insertis & Galsgaard \(2013\)](#) and [Nóbrega-Siverio et al. \(2016\)](#). The high brightening overlying the two vaults in the observations, in particular, is suggestive of the null point and CS complex in the models; the two vaults would then correspond to the domains occupied by the emerging plasma and the reconnected hot loops, respectively, in the models.
- The cool surge-like jets visible in the IRIS images may be the counterpart to the cool ejections that naturally accompany the flux emergence models. Further observed features that are present in flux emergence models are: the ejection of bright kernels from the region identified as the reconnection site, and the shift of the latter along the duration of the jet evolution in the direction of the cavity harboring hot loops in the EUV observations.

References

- Alexander, D. & Fletcher, L. 1999, *Sol. Phys.*, 190, 167
- Bagashvili, S. R., Shergelashvili, B. M., Japaridze, D. R., et al. 2018, *ApJ*, 855, L21
- Guo, Y., Démoulin, P., Schmieder, B., et al. 2013, *A&A*, 555, A19
- Innes, D. E., Cameron, R. H., & Solanki, S. K. 2011, *A&A*, 531, L13
- Joshi, R., Schmieder, B., Chandra, R., et al. 2017b, *Sol. Phys.*, 292, 152
- Li, H. D., Jiang, Y. C., Yang, J. Y., Bi, Y., & Liang, H. F. 2015, *Ap&SS*, 359, 4
- Moreno-Insertis, F. & Galsgaard, K. 2013, *ApJ*, 771, 20
- Moreno-Insertis, F., Galsgaard, K., & Ugarte-Urra, I. 2008, *ApJ*, 673, L211
- Nóbrega-Siverio, D., Martínez-Sykora, J., Moreno-Insertis, F., & Rouppe van der Voort, L. 2017, *ApJ*, 850, 153
- Nóbrega-Siverio, D., Moreno-Insertis, F., & Martínez-Sykora, J. 2016, *ApJ*, 822, 18
- Nóbrega-Siverio, D., Moreno-Insertis, F., & Martínez-Sykora, J. 2018, *ApJ*, 858, 8
- Pucci, S., Poletto, G., Sterling, A. C., & Romoli, M. 2012, *ApJ*, 745, L31
- Schmieder, B., Malherbe, J. M., Mein, P., et al. 1996, Vol. 111
- Shibata, K., Nozawa, S., & Matsumoto, R. 1992, *PASJ*, 44, 265